nature photonics

REVIEW ARTICLE

PUBLISHED ONLINE: 1 FEBRUARY 2011 | DOI: 10.1038/NPHOTON.2010.237

Antennas for light

Lukas Novotny[1]* and Niek van Hulst[2,3]

Optical antennas are devices that convert freely propagating optical radiation into localized energy, and vice versa. They enable the control and manipulation of optical fields at the nanometre scale, and hold promise for enhancing the performance and efficiency of photodetection, light emission and sensing. Although many of the properties and parameters of optical antennas are similar to their radiowave and microwave counterparts, they have important differences resulting from their small size and the resonant properties of metal nanostructures. This Review summarizes the physical properties of optical antennas, provides a summary of some of the most important recent developments in the field, discusses the potential applications and identifies the future challenges and opportunities.

Optical antennas, analogues of microwave and radiowave antennas, are a new concept in physical optics[1]. They are an enabling technology for manipulating and controlling optical radiation at subwavelength scales[2]. Optical antennas are the subject of a growing number of scientific studies, and hold promise for enhancing the efficiency of photodetection[3,4], light emission[5,6], sensing[7], heat transfer[8,9] and spectroscopy[10].

Traditionally, the field of optics and photonics deals with the control of propagating optical radiation using elements such as mirrors, lenses, fibres and diffractive elements. On the other hand, in the radiowave and microwave regime, using antennas of various designs to control electromagnetic fields on the subwavelength scale is a well-established technique. Antennas are pervasive in almost all areas of modern technology, ranging from satellite communications to baby phones.

Despite the widespread use of radiowave and microwave antennas, the optical analogue has not yet made its debut in technological applications, primarily because of its small size requirement. The characteristic dimensions of an antenna are of the order of the radiation wavelength, and for optical antennas this requires fabrication accuracies down to a few nanometres. However, this length scale has become increasingly accessible as the tools of nanoscience and nanotechnology have improved. Prototype optical antennas have been fabricated by top-down nanofabrication tools such as focused ion beam milling[11,12] or electron-beam lithography[13,14], and also by bottom-up self-assembly schemes[15,16]. It is evident that the fabrication of optical antenna structures provides an emerging opportunity for realizing new optoelectronic devices.

The objective of optical antenna design is equivalent to that of classical antenna design: to optimize the energy transfer between a localized source or receiver and the free-radiation field (Fig. 1). In certain recent studies, however, the term 'optical antenna' has clearly been stretched beyond its common definition in radiowave technology. An antenna is not simply a resonator or a strong scatterer. Instead, it is defined by its function, namely as a transducer between free radiation and localized energy. Its efficiency is defined by the degree of localization and the magnitude of transduced energy.

The term 'antenna' is used in a wide range of contexts, such as for tent posts, the beams of sailing boats or insect whiskers. The electromagnetic antenna, originally referred to as an 'aerial', is a transducer between electromagnetic waves and electric currents, and generally operates in the radiofrequency regime. In analogy with the electromagnetic antenna, we define the optical antenna as a device that converts freely propagating optical radiation into localized energy, and vice versa[1].

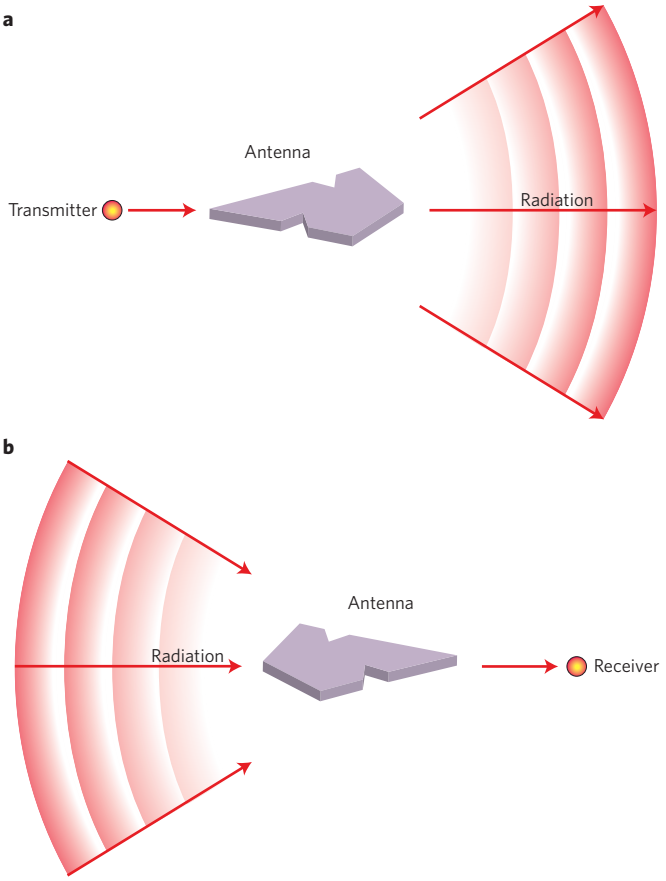

Figure 1 | Antenna design. a, Transmitting antenna. **b**, Receiving antenna. Arrows indicate the direction of energy flow. The two configurations are related by the principle of reciprocity. In spectroscopy and microscopy, the two antenna concepts are combined; that is, the antenna is used both as a receiver and as a transmitter.

The spatial extent of a receiver or transducer is commonly much smaller than the wavelength of radiation, λ, and is typically of

[1]Institute of Optics, University of Rochester, Rochester, New York 14627, USA. [2]Institut de Ciències Fotòniques, Mediterranean Technology Park, 08860 Castelldefels, Barcelona, Spain. [3]Institució Catalana de Recerca i Estudis Avançats, 08015 Barcelona, Spain. *e-mail: novotny@optics.rochester.edu

NATURE PHOTONICS DOI: 10.1038/NPHOTON.2010.237

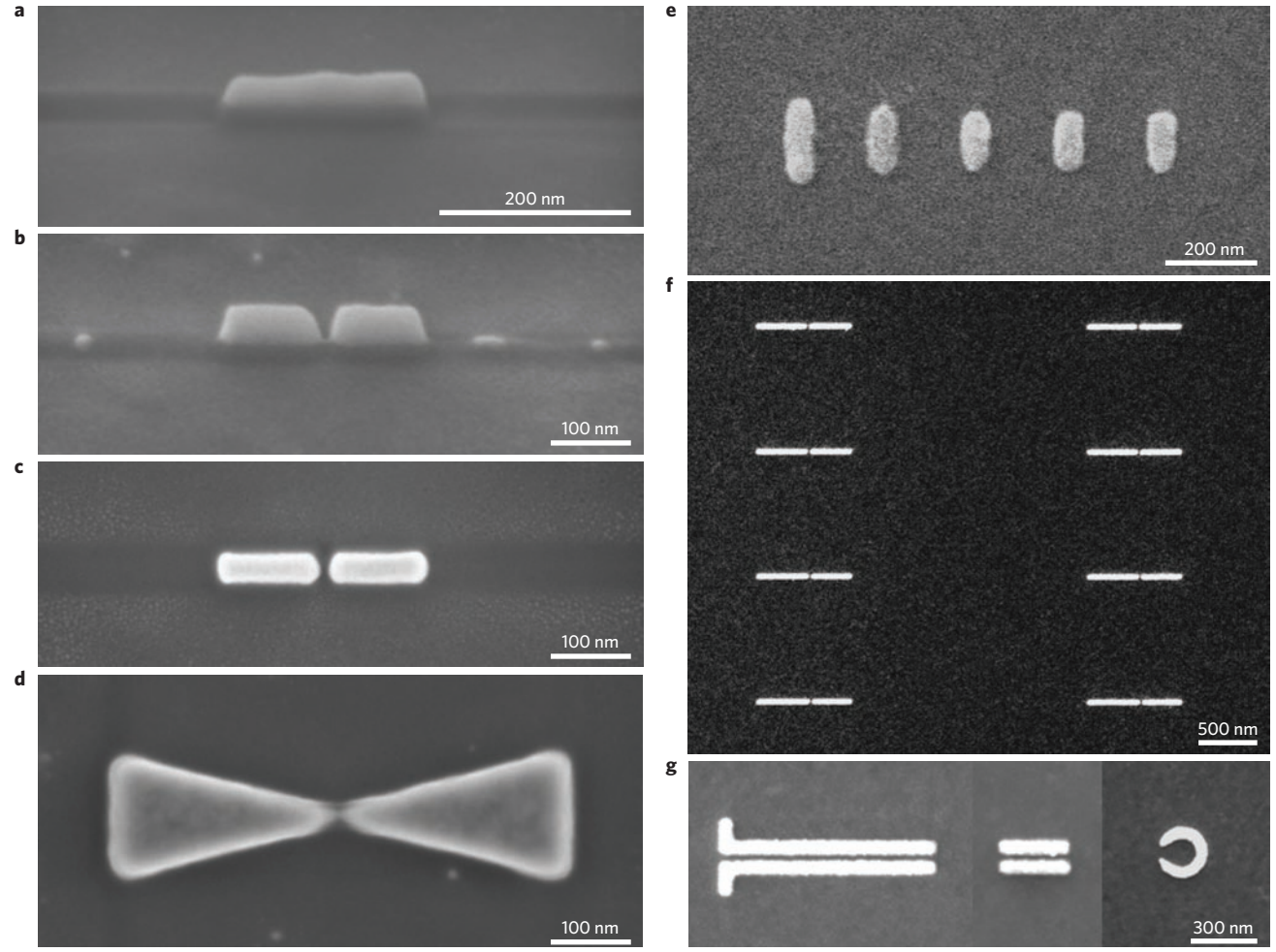

Figure 2 | Examples of top-down fabricated optical antennas. a–d, Various antennas with gap sizes down to ~10 nm, fabricated by focused ion beam milling. **e–g**, Yagi–Uda antenna (**e**), gap antennas (**f**) and plasmonic waveguide and split-ring resonator (**g**), fabricated by electron-beam lithography and subsequent lift-off.

the order of $\lambda/100$ (for a cell phone, $\lambda \sim 30$ cm). Translating this into the optical frequency regime, we require the dimensions of the receiver or transducer to be ~5 nm. For this length scale the light–matter interaction becomes quantized, and the sources and receivers become quantum objects such as molecules, atoms, ions or quantum dots.

In this Review we attempt to establish a terminology, provide an overview of ongoing research, summarize potential applications and discuss open questions and challenges.

History

The concept of the optical antenna has its roots in near-field optics[17]. In 1928, Edward Synge proposed the use of a colloidal gold particle for localizing optical radiation on a sample surface and thereby surpassing the diffraction limit in optical imaging[18]. Then, in 1985, John Wessel proposed for the first time that a gold particle could function as an antenna[19]. The first experimental demonstrations of this followed in 1995 by Dieter Pohl and Ulrich Fischer, who used a gold-coated polystyrene particle[20]. In the following years, optical antennas in the form of sharply pointed metal tips were used in near-field microscopy and spectroscopy[10]. These experiments gave birth to what is today known as 'tip-enhanced near-field optical microscopy'. It should be noted that antennas were used as whisker (Schottky) diodes for the detection and mixing of infrared radiation in as early as 1968[21–23]. These studies continued, and since then various infrared antenna geometries have been systematically investigated[24,25].

Bow-tie antennas were proposed as near-field optical probes in 1997, and initial proof-of-principle experiments have been performed in the microwave regime[26]. In follow-up experiments, bow-tie antennas were fabricated on the tips of atomic force microscopes[27]. After establishing the analogy between near-field optical probes and optical antennas[17], antenna structures were grown on the end faces of aperture-type near-field probes (also known as tip-on-aperture probes)[12,28]. Following these developments, several groups set out to explore various geometries of antenna, both experimentally and theoretically. As an example, Fig. 2 shows various antenna configurations fabricated by focused ion-beam milling and electron-beam lithography.

Surface plasmon resonances make optical antennas particularly efficient at selected frequencies — an attribute that also holds promise for biological sensing and detection[29–31]. In the 'Applications' section of this Review we describe some of the highlights of recent research into optical antennas, and discuss their potential applications. Recent reviews, tutorials and overviews can be found in refs 1,24,32–35.

Antenna parameters

A generic antenna problem is illustrated in Fig. 3. It consists of a transmitter and a receiver, both represented by dipoles **p**. The

antenna is introduced to enhance the transmission efficiency from the transmitter to the receiver. This enhancement can be achieved by increasing the total amount of radiation released by the transmitter, for which the antenna efficiency is a useful figure of merit:

$$\varepsilon_{\mathrm{rad}} = \frac{P_{\mathrm{rad}}}{P} = \frac{P_{\mathrm{rad}}}{P_{\mathrm{rad}} + P_{\mathrm{loss}}}$$

where P is the total power dissipated by the antenna, P_{rad} is the radiated power and P_{loss} is the power dissipated through other means, such as by absorption in the antenna. However, the transmission efficiency can also be improved by directing the radiation in the direction of the receiver. The efficiency for this process is represented by the directivity:

$$D(\theta,\phi) = \frac{4\pi}{P_{\mathrm{rad}}}\, p(\theta,\phi)$$

where the angles θ and ϕ represent the direction of observation and $p(\theta,\phi)$ is the angular power density. The combination of antenna efficiency and directivity is referred to as the antenna gain:

$$G = \frac{4\pi}{P}\, p(\theta,\phi) = \varepsilon_{\mathrm{rad}} D$$

By reciprocity, we can interchange the fields and sources in Fig. 3 to give $\mathbf{p}_1 \bullet \mathbf{E}_2 = \mathbf{p}_2 \bullet \mathbf{E}_1$, where $\mathbf{E}_1$ ($\mathbf{E}_2$) is the field of dipole $\mathbf{p}_1$ ($\mathbf{p}_2$) evaluated at the location of $\mathbf{p}_2$ ($\mathbf{p}_1$). A good transmitting antenna is therefore also a good receiving antenna. For a transmitter in the form of a two-state quantum emitter, reciprocity leads to a relationship between the emitter's excitation rate Γ_{exc} and its spontaneous emission rate Γ_{rad} (refs 1,2):

$$\frac{\Gamma_{\mathrm{exc},\theta}(\theta,\phi)}{\Gamma^{\mathrm{o}}_{\mathrm{exc},\theta}(\theta,\phi)} = \frac{\Gamma_{\mathrm{rad}}}{\Gamma^{\mathrm{o}}_{\mathrm{rad}}}\,\frac{D_{\theta}(\theta,\phi)}{D^{\mathrm{o}}_{\theta}(\theta,\phi)}$$

Here, the superscript 'o' refers to the absence of the antenna and the subscript 'θ' indicates the polarization state; that is, the electric field vector points in direction of the θ unit vector. An equivalent equation holds for polarization in the ϕ direction. Interestingly, excitation in a direction of high directivity allows the excitation rate to be enhanced more strongly than the radiative rate.

Another important antenna parameter is the antenna aperture, which is formally the same as the absorption cross-section σ. Let us consider a dipole-like receiver with a cross-section σ_{o} that is not coupled to an antenna. The unit vector in the direction of the absorption dipole axis is denoted as $\mathbf{n}_{\mathrm{p}}$ and the incident field at the location of the receiver is $\mathbf{E}_{\mathrm{o}}$. Once we couple the receiver to an antenna, the field at the receiver increases to $\mathbf{E}$ and the cross-section or antenna aperture becomes[1]

$$\sigma = \sigma_{\mathrm{o}} |\mathbf{n}_{\mathrm{p}} \bullet \mathbf{E}|^2 / |\mathbf{n}_{\mathrm{p}} \bullet \mathbf{E}_{\mathrm{o}}|^2 \qquad (1)$$

Thus, the aperture of an optical antenna scales with the local intensity enhancement factor. Theoretical and experimental studies have shown that intensity enhancements of 10^4–10^6 are readily achievable[14,36,37] and hence, for typical molecules with 'free-space' cross-sections of $\sigma_{\mathrm{o}} = 1\ \mathrm{nm}^2$, we find that a layer of molecules spaced 0.1–1 μm apart can absorb all of the incident radiation if each molecule is coupled to an optical antenna. Of course, this estimate ignores the coupling between antennas and therefore has limited validity.

Radiowave antennas have design rules that relate to the wavelength of incident radiation, λ. For example, a half-wave antenna has a length L of $\lambda/2$, and a Yagi–Uda antenna has separations between elements that correspond to certain fractions of λ (refs 38,39). Because all elements are proportional to λ, it is straightforward to scale the antenna design from one wavelength to another. However, this scaling fails at optical frequencies because the penetration of radiation into metals can no longer be neglected. Owing to the finite electron density, there is a delay between the driving field and the electronic response, resulting in a skin depth that is typically larger than the diameter of the antenna elements. As a consequence, electrons in metals do not respond to the wavelength λ of the incident radiation but to an effective wavelength λ_{eff}, which is determined by a simple linear scaling rule[40,41]:

$$\lambda_{\mathrm{eff}} = n_1 + n_2 \left(\frac{\lambda}{\lambda_{\mathrm{p}}}\right)$$

where n_1 and n_2 are geometric constants and λ_{p} is the plasma wavelength. According to this wavelength scaling rule, an optical half-wave antenna is not $\lambda/2$ in length but a shorter length of $\lambda_{\mathrm{eff}}/2$. The difference between λ and λ_{eff} depends on geometric factors, but is typically in the range of 2–5 for most of the metals used as optical antennas.

Metals might not be the right choice of material for antenna elements with diameters of less than 5 nm, as the conductivity drops considerably. Carbon nanotubes are better conductors than metals at diameters of <5 nm (ref. 42). On the very small scale, therefore, carbon materials such as graphene and nanotubes might become the building blocks of choice for optical antennas[43,44]. Reducing the dimensions even further reaches the molecular scale, where the design of optical antennas could draw inspiration from biology. For example, in light-harvesting proteins, chlorophyll molecules arrange in favourable configurations to operate as one coherent entity[45].

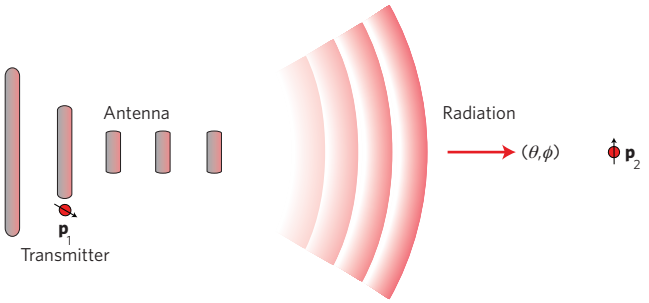

Figure 3 | An antenna enhances the transmission efficiency from the transmitter to the receiver. The transmitter is modelled by the dipole $\mathbf{p}_1$, and the receiver by the dipole $\mathbf{p}_2$.

Applications

In this section we discuss some of the emerging applications of optical antennas. The objective of this discussion is not to present an exhaustive review, but rather to touch on particularly promising selected topics.

Photodetection and photovoltaics. The application of optical antennas in photodetectors is particularly promising. The main reason is that, according to equation (1), an optical antenna increases the absorption cross-section and hence the light flux that impinges on a detector, giving it a clear signal-to-noise advantage.

Our ability to shrink the detector area A has so far been limited by the diffraction limit of focusing elements. Furthermore, the thickness of a detector is typically limited by the absorption

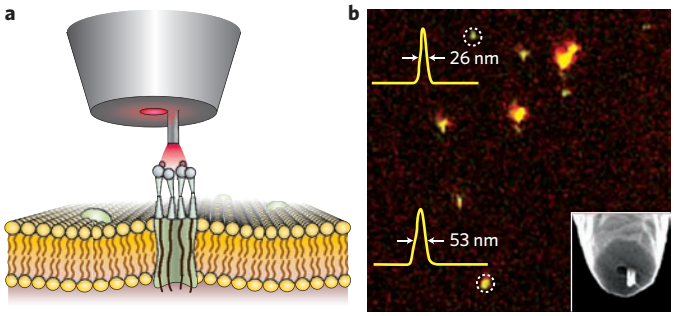

Figure 4 | Biological imaging with optical antennas. a, Schematic illustration, not to scale. **b**, Fluorescently labelled antibodies imaged by the antenna probe. Cross-sections of the two circled features in **b** show responses of 26 nm and 53 nm (full-width at half-maximum). Figure reproduced with permission from ref. 31, © 2010 Wiley.

depth of the detector material. Optical antennas can be used in a photodetector to further reduce its critical dimensions and improve performance metrics such as the signal-to-noise ratio, power consumption and speed[3,25,29,46]. Using antennas reduces the detector area 100-fold, thus gaining at least an order of magnitude in sensitivity. The speed of a photodetector depends on the time it takes for photogenerated carriers to traverse the circuit, which scales with the detector size. Similar considerations hold for the power consumption. Because the dark current i_D of a photodetector scales with the detector area A we find that both the noise current $i_N = (2e\, i_D\, \Delta f)^{1/2}$ and the noise equivalent power NEP = $(i_N/\eta)\,(h\nu/e)$ scale with the square root of A. Here, η is the quantum efficiency, ν is the frequency and Δf is the bandwidth. The NEP corresponds to the lowest power a detector can detect with a signal-to-noise ratio of 1. To eliminate the dependence on detector area, one defines the detectivity $D^* = (A\Delta f)^{1/2}/\mathrm{NEP}$, with units of cm $\mathrm{Hz}^{1/2}$ W^{-1} (known as the Jones). Recent studies have reported values of NEP = 1.53 nW and $D^* = 2.15 \times 10^6$ Jones for antenna-coupled infrared detectors based on metal–oxide–metal diodes[47]. Current research is aimed at improving these values and extending operation to optical frequencies.

Optical antennas have also been explored for enhancing the efficiency of photovoltaic devices, particularly for solar energy harvesting[1,48]. The main emphasis is on reducing the photovoltaic layer thickness in thin-film devices to lower the carrier collection length and reduce impurity recombination, while keeping the optical absorption constant[48].

Antenna probes for nano-imaging. Over the past decade, optical microscopy has reached the nanoscale through techniques such as stimulated emission depletion (STED) microscopy, photoactivatable localization microscopy (PALM) and stochastic optical reconstruction microscopy (STORM)[49–53]. All of these far-field lens-based methods reveal 20–50 nm features, and rely on the fluorescence detection of dyes with suitable photodynamic properties for depletion or photoswitching. PALM and STORM in particular are finding rapid acceptance in biological applications.

Optical antennas, when used in scanning probe arrangement, yield a spatial response function on the 10–50 nm scale, independent of the nature and photophysics of the sample; this is in contrast with far-field approaches. Several types of sharp tip were initially exploited to achieve a locally 'tip-enhanced' response, with resolutions of 10–30 nm achieved in certain cases[28,54–56]. Dieter Pohl[17] was the first to point out the analogy between optical probes and optical antennas, following which scanning antenna probes were steadily investigated. The first of such studies involved attaching colloidal spherical gold particles (~80 nm), tuned to resonance with the incident light, to glass probes. Scanning these resonant spheres close to single fluorescent molecules was found to both enhance fluorescence and reduce lifetime (up to 20 times)[16,57,58]. Hoeppener *et al.*[30] used such a nanoprobe to achieve a resolution of ~50 nm in the imaging of single calcium channel proteins on red blood cell membranes. Achieving a higher spatial resolution requires antennas with strongly localized fields[59], smaller particles, sharper antenna ends or a narrower feed gap. Taminiau *et al.*[12] used top-down ion-beam milling to carve an 80 nm aluminium rod on a probe, which then functioned as a monopole antenna. Recently, such monopole antennas have been used to image single proteins and nanodomains with 30 nm resolution in cell membranes in liquid (Fig. 4)[31].

The bow-tie antenna design is particularly promising for efficient field confinement in the antenna gap. Several interesting bow-tie antenna probes have been fabricated by ion-beam milling and electron-beam deposition[27,60], although so far without routine nanoscale imaging capability. Studies into the use of colloidal particles are now resulting in multiple particle probes (Fig. 5); for example, nanoparticle pairs have been shown to display strong nonlinear responses (particularly third order) such as four-wave mixing[61], in which the localized four-wave mixing source is ideal for background-free nanoscale imaging. Aside from colloidal spheres, 'nanostars' with multiple nanoprotrusions are attracting attention for their strongly localized fields[62]; a nanostar attached to a scanning probe might be able to push optical imaging beyond 10 nm resolution. Clearly both the top-down and bottom-up methods are progressing fast, and several creative antenna probes will be realized in the near future. In contrast with PALM and STORM, which rely on particular photoswitching properties, the antenna approach provides true field localization, which can be applied to any dye, fluorescent protein or quantum dot. This approach might even be applied to Raman spectroscopy and hyperspectral imaging. Finally, the manipulation of photodynamic properties by antenna control will allow original approaches for near-field localization microscopy — an avenue that is yet unexplored.

Nonlinear signal conversion. The strong optical nonlinearities of metals bring many opportunities for nanoscale photonic devices. Research into active and nonlinear plasmonics is only just beginning. Among the potential applications are signal amplification and optical frequency conversion. The nonlinearities of metals are particularly strong compared with dielectrics. For example, the third-order nonlinear susceptibility of gold ($\chi^{(3)} < 1$ nm^2 V^{-2})[63] is more than three orders of magnitude larger than the susceptibility of nonlinear crystals such as KDP, KTP or $LiNbO_3$. Nonlinear optical antennas hold promise for generating and controlling this nonlinear response on a subwavelength scale. For example, it has been demonstrated that controlling the gap between the nanoparticles in a gold nanoparticle dimer allows the intensity of the nonlinear frequency conversion to be tuned over four orders of magnitude[61,64]. So far, the nonlinear processes that have been explored in metal nanostructures include harmonic generation[65–67], two-photon excited luminescence[13,68,69] and nonlinear four-wave mixing[61,64]. The design and optimization of nonlinear optical antennas is challenging because of the different wavelengths that are involved. Nonlinear optical antennas open the door for exploiting frequency-selective local interactions across the entire visible and infrared spectrum using a single-frequency excitation source.

Information processing. There is an upper limit to the performance of optical components[70]. A minimum volume must be ensured to guarantee the necessary number of modes for information to be processed. The limit is valid for multiple scattering events and for linear interactions. The minimum volume scales with the dielectric constant of a material, and hence it can be reduced by using metallic

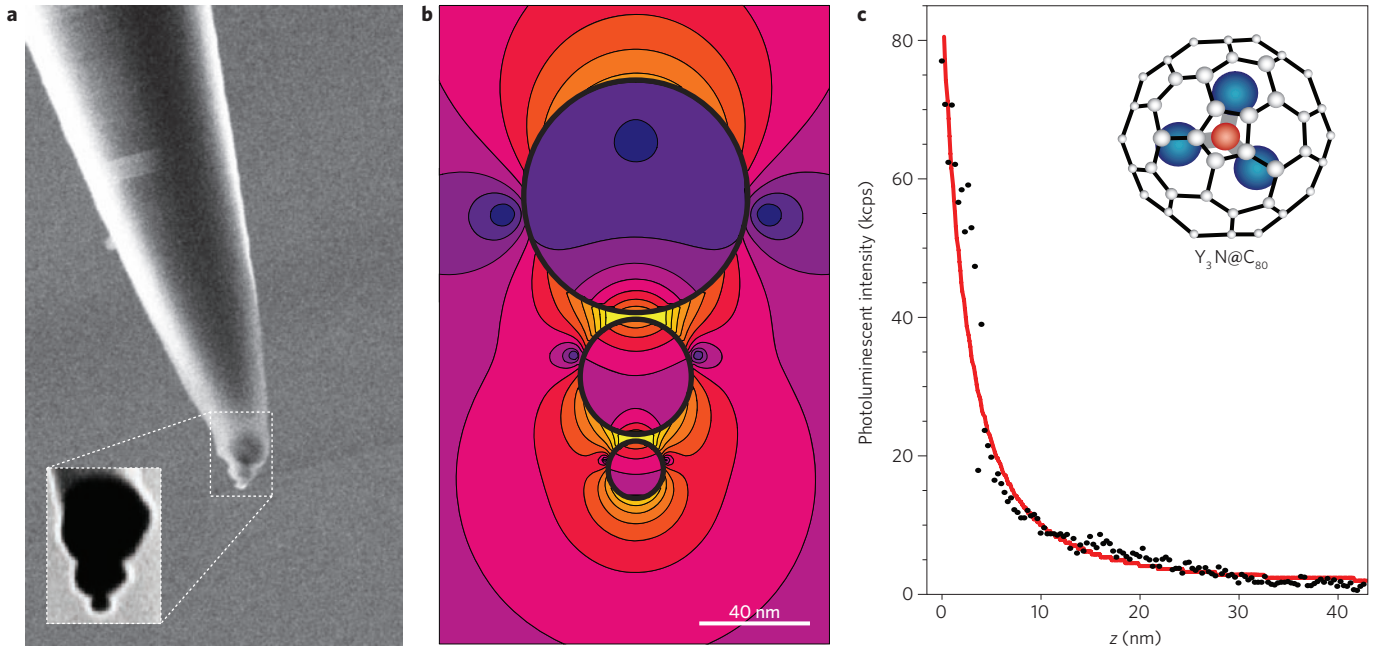

Figure 5 | Example of a bottom-up fabricated optical antenna. a, SEM image of a gold trimer antenna consisting of gold nanoparticles supported by a dielectric tip. The particle sizes are 180, 90 and 50 nm. **b**, Computed intensity near a trimer antenna irradiated at a wavelength of 650 nm. Adjacent contour lines differ by a factor of two in intensity. **c**, Fluorescence from a metallofullerene ($Y_3N@C_{80}$, pictured inset) as a function of its distance from a gold nanoparticle antenna. Because of the low intrinsic quantum yield of $Y_3N@C_{80}$, the antenna enhances the fluorescence by two orders of magnitude. Figure **c** reproduced with permission from ref. 98, © 2010 ACS.

structures such as optical antennas. Furthermore, as discussed previously, metals have high intrinsic nonlinearities and therefore hold promise for signal processing beyond the linear limit.

Super-bright single-photon sources. A single dipole emitter close to an optical antenna will experience a modified photonic mode density. A spectacular enhancement — up to ~500 times — can occur when the antenna is resonant with the dipole transition, such as in a resonant antenna–molecule system. The radiative rate Γ_{rad} becomes competitive with the non-radiative rate $\Gamma_{non\text{-}rad}$, therefore boosting the emission to 10–50 ps Rabi periods, while the quantum efficiency (the relative fraction of radiative decay) approaches unity — true super-emission with a picosecond decay time. The enhanced radiative rate is a strong function of distance and orientation with respect to the nanoparticle, requiring positional control on a subnanometre scale. Bright molecule emission with a lifetime of ~20 ps was recently observed in the gap of a bow-tie antenna for the first time[14]. Such high quantum efficiency super-bright single-photon sources are ideal candidates for applications in quantum optics. When combined with directional antennas, one can even foresee the efficient coupling of quantum sources over long distance. It is interesting to note that optical antennas that confine light to nanometre-scale hot-spots have a reasonably high light storage capacity; the ratio of quality factor and volume is comparable to the value for good microcavities (~10^6 μm^{-3}). Optical antennas might therefore allow the strong coupling regime to be achieved through an alternative route that does not involve microcavities.

Challenges and outlook

Many different optical antenna geometries have been studied over the past few years. Among them are bow-tie antennas[14,27,69], half-wave antennas[3,13,40,41,71–74], monopole antennas[12,75], particle antennas[15,16,57,58], Yagi–Uda antennas[38,39,75–77], gap antennas[5,11,13,73,74], slot antennas[78], cross antennas[79] and patch antennas[80]. Although these studies established important groundwork, several challenges remain that must be addressed before optical antennas can become a widely deployable technology.

Pursuing the radiofrequency antenna analogy. How far has the optical analogy of radiofrequency antennas been accomplished? Top-down nanofabrication tools such as electron-beam lithography and ion-beam milling have been widely used to downscale established radiofrequency antenna configurations to the optical frequency regime. However, unlike radiofrequency antennas, which are locally driven at the feed gap, early optical antennas were driven from the far-field. Antenna-mediated transduction has been explored mainly for infrared detection using, for example, a slot antenna[81] or an open-sleeve dipole antenna (Fig. 6)[3]. However, the large variety of optimized radiofrequency antennas is still waiting to be explored at optical frequencies. For directional emission (or detection), obvious candidates are traditional loop and travelling-wave antennas such as the long-wire Beverage antenna, which should be relatively simple to scale down to the submicrometre scale. So far, however, compact multi-element unidirectional antennas have received the most attention. In particular, the elegant Yagi–Uda design was used in several theoretical papers[75–77], in which it was shown that the emission of an optical source at the feed element can be fully directed in a single cone. Recently the first directional scattering from an array of optical Yagi–Uda antennas was demonstrated experimentally[38,39]. The road is open to realizing compact efficient photon sources with controlled narrow-emission angles. Through reciprocity one could drive the system in receiving mode by excitation into the narrow acceptance cone.

Modern radiofrequency antennas are highly optimized in terms of their bandwidth and size. Cellular phones often contain super-compact monopole antennas with fractal-like designs for broadband operation. The concept of fractal design in optics was first suggested by Stockmann[82] and co-workers in a self-similar chain of particles (Fig. 5), exploiting the multiplicative cascade effect to achieve nano-focusing at the smallest particle. One can pursue this idea, through

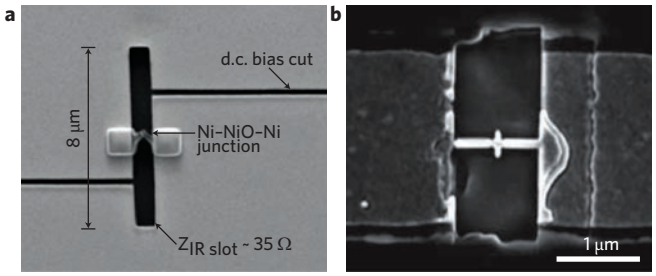

Figure 6 | SEM images of two types of infrared antennas. a, Slot antenna coupled to a Ni–NiO–Ni diode for electrical read-out. **b**, Open-sleeve dipole antenna coupled to a germanium photodetector. Figure reproduced with permission from: **a**, ref. 81, © 2005 AIP; **b**, ref. 3, © 2008 NPG.

modern fractal antenna designs such as the Sierpinski carpet[83], for the broadband capture of light and efficient channelling to a singular point. In practice the challenge lies in attaining the smallest achievable feature size, which sets the operational frequency limit of such designs.

Control of antenna directionality is generally achieved by regulating the impedance match (see below) or by using phased array geometries, which tune the phase between the constituting antenna elements and thereby allow rapid steering of beams. Optical phase antennas, which consist of a particle array with dedicated spacing between the sources, have been proposed to achieve near-field focusing[84], and focusing from particle and hole arrays has been observed[85]. However, the phase control of coupled optical antenna elements is a challenge yet to be explored. Comparisons are naturally made with existing phased-array optics based on spatial light modulators, in which the source elements have dimensions of many optical wavelengths. A phased optical antenna array could miniaturize spatial light modulator technology while simultaneously making the connection to the near-field with nanoscale sources/detectors. One can foresee an array of coherently coupled photon sources whose emission direction can be dynamically steered by phase control.

Impedance matching. A major challenge in the design of optical antennas is impedance matching between the antenna and the source. For a source in the form of an atom or molecule, we find a largely reactive impedance of roughly 1 MΩ, which follows from treating the atom/molecule as a plate capacitor of area 0.2 nm × 0.2 nm, and a plate separation of similar dimensions. On the other hand, the impedance of a typical metal nanostructure is mostly Ohmic and is extremely small (~3 Ω for a linear half-wave antenna)[1,40]. It is currently unclear how to compensate for this large impedance mismatch. Impedance matching is important for efficient coupling between the source and the radiation field. The first steps have been undertaken[71,86], and it has been shown that controlling the impedance in the feed-gap of a half-wave antenna allows the antenna resonance to be spectrally tuned[72,74,87].

Because of spontaneous emission, the impedance of an atom cannot be purely imaginary. Radiation losses must be accounted for by the real part of the impedance or, equivalently, by the radiation resistance. To efficiently radiate, the excited state lifetime of an atom must be small. In other words, the more decay channels there are, the easier it is for an excited atom to return to its ground state. The radiation resistance must therefore be related to the local density of electromagnetic states, ρ (refs 1,88). Coupling to an optical antenna increases ρ and makes the atom or molecule a more efficient emitter[14,16,57,58].

Electro-optical transduction. In the traditional radiofrequency and microwave regime, antennas are usually used to convert electromagnetic radiation into electric currents, and vice versa. However, most of the optical antennas studied so far operate on a 'light-in, light-out' basis. There are only a few studies that report the antenna-assisted conversion of optical radiation into photocurrents[3,46]. Antenna-assisted electro-optical transduction can draw inspiration from high-frequency devices such as infrared whisker diodes based on metal–oxide–metal junctions[21,23], and from photon emission in scanning tunnelling microscopy[89,90]. Such infrared whisker diodes provide a route towards receiving electro-optical antennas[24], whereas scanning tunnelling microscopy defines a possibility for transmitting electro-optical antennas. The problem in metal–oxide–metal diodes is the high-frequency cut-off, which depends on the capacitance of the metal–oxide–metal junction[81]. Reliable operation has not yet been extended into the optical frequency regime. On the other hand, in photon emission scanning tunnelling microscopy, electrons excite surface plasmons, which then decay radiatively[91,92]. This process has a low efficiency, and reliable operation at the device level has not yet been established. Nevertheless, emerging nanofabrication tools make it possible to engineer and control ever-smaller length scales, and it can be expected that electro-optical antennas based on electron–plasmon coupling will be realized at some point.

Selection rules. We have already pointed out several important differences between optical antennas and classical radiowave antennas. For example, at optical frequencies, the penetration of radiation into metals can no longer be neglected, and consequently optical antennas respond to a scaled, effective wavelength rather than to the wavelength of the incoming radiation. In addition, at optical frequencies metals are very nonlinear materials, which makes it possible to mix and convert different frequencies. Finally, and most importantly, the localized fields near optical antenna structures have spatial dimensions that approach the length scale of atomic/molecular quantum wavefunctions. This opens up interaction channels that are forbidden by standard electric dipole selection rules[1]. Also, the strong field localization near an optical antenna gives rise to photon momenta that are of the order of the momenta of electrons in matter, and can therefore give rise to traditionally momentum-forbidden transitions. Although near-field interactions beyond the dipole selection rules have been the subject of theoretical studies[93], they still wait for systematic experimental verification. One-photon excited photoluminescence from metal nanostructures is believed to have its origin in momentum-forbidden transitions[94], and the same process is believed to be involved in photoelectron emission from roughened surfaces[95]. Because near-field interactions open up transition channels that are inaccessible through radiative excitation, they hold promise for boosting the sensitivity of photodetection and optical sensing.

Reproducibility and repeatability. Any progress in the application of optical antennas depends critically on the capacity to fabricate an optimal geometry with sufficient material quality and nanoscale accuracy. Traditionally, the bottom-up colloidal synthesis approach has provided high-quality crystalline metallic nanoparticles of controllable shape and size to within a few nanometres. The colloidal particles show high-quality resonances ($Q > 10$) approaching the limits set by the metal dielectric properties[96]. In addition, core–shell, triangle, pentagon and even star-like particles have been synthesized[62,97]. Arranging colloidal particles to compose a designed antenna geometry is still a challenge, although antenna probes have been fabricated by picking up individual or multiple gold nanoparticles[16,57,98] (Fig. 5). All this repeatability depends largely on the researcher's skills and patience.

Today, extended arrays of optical antennas (usually made of gold or silver) are routinely fabricated by top-down electron-beam lithography in a photoresist, followed by development, metal coating and subsequent metal lift-off. Although an accuracy of 10–20 nm has been achieved (Fig. 2), the metals are generally polycrystalline, with 10–30 nm grains. As a result, the resonances are generally of low quality ($Q \sim 5$), and the properties of individual antennas can be affected by the nanoscale arrangement of just one or two grains.

The direct carving of antennas by focused ion beam milling is a good alternative to electron-beam lithography, particularly for more complex three-dimensional structures or dedicated post-processing steps[12]. Again, reproducibility is a matter of patience. The implantation of gallium ions seems to have an insignificant effect on antenna resonance. Ion-milling could be performed on sheets of crystalline gold or silver, thereby opening the route to high-quality single-crystalline complex antenna geometries[99].

Although techniques in the field of antenna nanofabrication have progressed rapidly, the major hurdle now is how to couple antennas to active optical sources such as molecules, quantum dots and nitrogen–vacancy centres. Most work so far has relied on randomly depositing such sources onto an array of antennas, either as a monolayer or as a low 'single-molecule' concentration. Post-selection can be used to identify 'hot spots', and indeed orders of magnitude in antenna enhancement have been observed[14], although the exact molecule–antenna arrangement usually remains unknown. Vice versa, colloidal antennas have been spread on pre-patterned samples[46]. Much more direct control has been achieved by scanning antenna probes in close proximity to molecules or quantum dots, where the relative position and orientation are both fully controlled, giving independent insight on the excitation enhancement and how the emission is modified[2,16,57].

For applications, one ideally envisions arrays of antennas, each driven by an optical source (or read-out by an optical detector) at its optimal feed point. Clearly directed nanopositioning of single quantum emitters (detectors) with full control of both location and orientation relative to the antenna remains the challenge for future functional applications.

Conclusions

Optical antennas have emerged as the dominant tool for manipulating light at the nanometre scale, while also providing optimal control of transduction in the far-field. Current research into optical antennas is being driven in particular by advances in nanofabrication and analogies with radiofrequency antennas. Although many antenna configurations are now being realized at optical frequencies, it is interesting to see how antenna concepts such as impedance matching are being redefined for optical sources such as atoms and molecules. Optical antennas connect to quantum systems and pure photon sources, and in doing so involve interesting new physics such as the breaking of selection rules and alternative routes for strong coupling. Concepts of directed emission and directed reception can now be applied to photon emitters. Once the fabrication techniques have been mastered, a wide range of applications will emerge, including controlled single-photon sources for quantum information, light harvesting, energy conversion, efficient biosensors, data storage[100,101], nanoscale optical circuitry and optical imaging beyond 10 nm resolution.

References

1. Bharadwaj, P., Deutsch, B. & Novotny, L. Optical antennas. *Adv. Opt. Photon.* **1,** 438–483 (2009).
2. Taminiau, T. H., Stefani, F. D. & van Hulst, N. F. Enhanced directional excitation and emission of single emitters by a nano-optical Yagi–Uda antenna. *Opt. Express* **16,** 10858–10866 (2008).
3. Tang, L. *et al.* Nanometre-scale germanium photodetector enhanced by a near-infrared dipole antenna. *Nature Photon.* **2,** 226–229 (2008).
4. Cao, L., Park, J.-S., Fan, P., Clemens, B. & Brongersma, M. L. Resonant Germanium nanoantenna photodetectors. *Nano Lett.* **10,** 1229–1233 (2010).
5. Cubukcu, E., Kort, E. A., Crozier, K. B. & Capasso, F. Plasmonic laser antenna. *Appl. Phys. Lett.* **89,** 093120 (2006).
6. Pillai, S., Catchpole, K., Trupke, T. & Green, M. Surface plasmon enhanced silicon solar cells. *J. Appl. Phys.* **101,** 093105 (2007).
7. Anker, J. N. *et al.* Biosensing with plasmonic nanosensors. *Nature Mater.* **7,** 442–453 (2008).
8. DeWilde, Y. *et al.* Thermal radiation scanning tunnelling microscopy. *Nature* **444,** 740 (2006).
9. Schuller, J. A., Taubner, T. & Brongersma, M. L. Optical antenna thermal emitters. *Nature Photon.* **3,** 658–661 (2009).
10. Novotny, L. & Stranick, S. J. Near-field optical microscopy and spectroscopy with pointed probes. *Ann. Rev. Phys. Chem.* **57,** 303–331 (2006).
11. Muehlschlegel, P., Eisler, H.-J., Martin, O. J. F., Hecht, B. & Pohl, D. W. Resonant optical antennas. *Science* **308,** 1607–1609 (2005).
12. Taminiau, T. H. *et al.* Resonance of an optical monopole antenna probed by single molecule fluorescence. *Nano Lett.* **7,** 28–33 (2007).
13. Ghenuche, P., Cherukulappurath, S., Taminiau, T. H., van Hulst, N. F. & Quidant, R. Spectroscopic mode mapping of resonant plasmon nanoantennas. *Phys. Rev. Lett.* **101,** 116805 (2008).
14. Kinkhabwala, A. *et al.* Large single-molecule fluorescence enhancements produced by a bowtie nanoantenna. *Nature Photon.* **3,** 654–657 (2009).
15. Kalkbrenner, T. *et al.* Optical microscopy via spectral modifications of a nanoantenna. *Phys. Rev. Lett.* **95,** 200801 (2005).
16. Anger, P., Bharadwaj, P. & Novotny, L. Enhancement and quenching of single molecule fluorescence. *Phys. Rev. Lett.* **96,** 113002 (2006).
17. Pohl, D. W. Near-field optics seen as an antenna problem in *Near-field Optics, Principles and Applications* (eds Zhu, X. & Ohtsu, M.) 9–21 (World Scientific, 2000).
18. Novotny, L. Effective wavelength scaling for optical antennas. *Phys. Rev. Lett.* **98,** 266802 (2007).
19. Wessel, J. Surface-enhanced optical microscopy. *J. Opt. Soc. Am. B* **2,** 1538–1540 (1985).
20. Fischer, U. C. & Pohl, D. W. Observation on single-particle plasmons by near-field optical microscopy. *Phys. Rev. Lett.* **62,** 458–461 (1989).
21. Hocker, L. O., Sokoloff, D. R., V. Daneu, A. S. & Javan, A. Frequency mixing in the infrared and far-infrared using metal-to-metal point contact diode. *Appl. Phys. Lett.* **12,** 401–402 (1968).
22. Fetterman, H. R., Clifton, B. J., Tannenwald, P. E. & Parker, C. D. Submillimeter detection and mixing using Schottky diodes. *Appl. Phys. Lett.* **24,** 70–72 (1974).
23. Fetterman, H. R. *et al.* Far-IR heterodyne radiometric measurements with quasioptical Schottky diode mixers. *Appl. Phys. Lett.* **33,** 151–153 (1978).
24. Alda, J., Rico-Garcia, J., Lopez-Alonso, J. & Boreman, G. Optical antennas for nano-photonic applications. *Nanotechnology* **16,** S230–S234 (2005).
25. Gonzalez, F. & Boreman, G. Comparison of dipole, bowtie, spiral and log-periodic IR antennas. *Infrared Phys. Technol.* **146,** 418–428 (2004).
26. Grober, R. D., Schoelkopf, R. J. & Prober, D. E. Optical antenna: towards a unity efficiency near-field optical probe. *Appl. Phys. Lett.* **70,** 1354–1356 (1997).
27. Farahani, J. N., Pohl, D. W., Eisler, H.-J. & Hecht, B. Single quantum dot coupled to a scanning optical antenna: A tunable superemitter. *Phys. Rev. Lett.* **95,** 017402 (2005).
28. Frey, H. G., Witt, S., Felderer, K. & Guckenberger, R. High-resolution imaging of single fluorescent molecules with the optical near-field of a metal tip. *Phys. Rev. Lett.* **93,** 200801 (2004).
29. Schuller, J. A. *et al.* Plasmonics for extreme light concentration and manipulation. *Nature Mater.* **9,** 193–204 (2010).
30. Hoeppener, C. & Novotny, L. Antenna-based optical imaging of single Ca^{2+} transmembrane proteins in liquids. *Nano Lett.* **8,** 642–646 (2008).
31. van Zanten, T. S., Lopez-Busquets, M. J. & Garcia-Parajo, M. F. Imaging individual proteins and nanodomains on intact cell membranes with a probe-based optical antenna. *Small* **6,** 270–275 (2010).
32. Hecht, B., Muehlschlegel, P., Farahani, J., Eisler, H.-J. & Pohl, D. W. Resonant optical antennas and single emitters in *Tip Enhancement* (eds Kawata, S. & Shalaev, V. M.) 275–307 (Elsevier, 2007).
33. Gevaux, D. Nano-antenna picks up green light. *Nature Photon.* **1,** 90 (2007).
34. Novotny, L. Optical antennas tuned to pitch. *Nature* **455,** 879–880 (2008).
35. Greffet, J.-J. Nanoantennas for light emission. *Science* **308,** 1561–1563 (2005).
36. Novotny, L., Bian, R. X. & Xie, X. S. Theory of nanometric optical tweezers. *Phys. Rev. Lett.* **79,** 645–648 (1997).
37. Crozier, K. B., Sundaramurthy, A., Kino, G. S. & Quate, C. F. Optical antennas: Resonators for local field enhancement. *J. Appl. Phys.* **94,** 4632–4642 (2003).
38. Curto, A. G. *et al.* Unidirectional emission of a quantum dot coupled to a nanoantenna. *Science* **329,** 930–933 (2010).
39. Kosako, T., Kadoya, Y. & Hofmann, H. F. Directional control of light by a nano-optical Yagi–Uda antenna. *Nature Photon.* **4,** 312–315 (2010).
40. Novotny, L. The history of near-field optics. *Prog. Opt.* **50,** 137–180 (2007).
41. Bryant, G. W., de Abajo, F. J. G. & Aizpurua, J. Mapping the plasmon resonances of metallic nanoantennas. *Nano Lett.* **8,** 631–636 (2008).
42. Sfeir, M. Y. *et al.* Optical spectroscopy of individual single-walled carbon nanotubes of defined chiral structure. *Science* **312,** 554–556 (2006).
43. Burke, P. J., Li, S. & Yu, Z. Quantitative theory of nanowire and nanotube antenna performance. *IEEE Trans. Nanotech.* **5,** 314–334 (2006).
44. Hao, J. & Hanson, G. W. Infrared and optical properties of carbon nanotube dipole antennas. *IEEE T. Nanotechnol.* **5,** 766–775 (2006).

45. Blankenship, R., Madigan, M. T. & Bauer, C. E. (eds) *Anoxygenic Photosynthetic Bacteria* (Kluwer, 1995).
46. Falk, A. L. *et al.* Near-field electrical detection of optical and single-plasmon sources. *Nature Phys.* **5,** 475–479 (2009).
47. Bean, J. A., Tiwari, B., Bernstein, G. H., Fay, P. & Porod, W. Thermal infrared detection using dipole antenna-coupled metal-oxide-metal diodes. *J. Vac. Sci. Technnol. B* **27,** 11–14 (2009).
48. Atwater, H. A. & Polman, A. Plasmonics for improved photovoltaic devices. *Nature Mater.* **9,** 205–213 (2010).
49. Hell, S. W. & Wichmann, J. Breaking the diffraction resolution limit by stimulated emission: Stimulated-emission-depletion fluorescence microscopy. *Opt. Lett.* **19,** 780–782 (1994).
50. Westphal, V. & Hell, S. W. Nanoscale resolution in the focal plane of an optical microscope. *Phys. Rev. Lett.* **94,** 143903 (2005).
51. Betzig, E. Proposed method for molecular optical imaging. *Opt. Lett.* **20,** 237–239 (1995).
52. Betzig, E. *et al.* Imaging intracellular fluorescent proteins at nanometer resolution. *Science* **313,** 1642–1645 (2006).
53. Rust, M., Bates, M. & Zhuang, X. Sub-diffraction limit imaging by stochastic optical reconstruction microscopy (storm). *Nat. Methods* **3,** 793–796 (2006).
54. Sanchez, E. J., Novotny, L. & Xie, X. S. Near-field fluorescence microscopy based on two-photon excitation with metal tips. *Phys. Rev. Lett.* **82,** 4014–4017 (1999).
55. Gerton, J. M., Wade, L. A., Lessard, G. A., Ma, Z. & Quake, S. R. Tip-enhanced fluorescence microscopy at 10 nanometer resolution. *Phys. Rev. Lett.* **93,** 180801 (2004).
56. Hartschuh, A., Sanchez, E., Xie, X. & Novotny, L. High-resolution near-field Raman microscopy of single-walled carbon nanotubes. *Phys. Rev. Lett.* **90,** 095503 (2003).
57. Kuehn, S., Hakanson, U., Rogobete, L. & Sandoghdar, V. Enhancement of single-molecule fluorescence using a gold nanoparticle as an optical nanoantenna. *Phys. Rev. Lett.* **97,** 017402 (2006).
58. Bharadwaj, P. & Novotny, L. Spectral dependence of single molecule fluorescence enhancement. *Opt. Express* **15,** 14266–14274 (2007).
59. Garcia-Parajo, M. F. Optical antennas focus in on biology. *Nature Photon.* **2,** 201–203 (2008).
60. Weber-Bargioni, A. *et al.* Functional plasmonic antenna scanning probes fabricated by induced-deposition mask lithography. *Nanotechnology* **21,** 065306 (2010).
61. Palomba, S. & Novotny, L. Near-field imaging with a localized nonlinear light source. *Nano Lett.* **9,** 3801–1804 (2009).
62. Rodriguez-Lorenzo, L. *et al.* Zeptomol detection through controlled ultrasensitive surface enhanced Raman scattering. *J. Am. Chem. Soc.* **131,** 4616–4618 (2009).
63. Renger, J., Quidant, R., Hulst, N. V. & Novotny, L. Surface enhanced nonlinear four-wave mixing. *Phys. Rev. Lett.* **104,** 046803 (2010).
64. Danckwerts, M. & Novotny, L. Optical frequency mixing at coupled gold nanoparticles. *Phys. Rev. Lett.* **98,** 026104 (2007).
65. Bouhelier, A., Beversluis, M., Hartschuh, A. & Novotny, L. Near-field second-harmonic generation induced by local field enhancement. *Phys. Rev. Lett.* **90,** 013903 (2003).
66. Lippitz, M., van Dijk, M. A. & Orrit, M. Third-harmonic generation from single gold nanoparticles. *Nano Lett.* **5,** 799–802 (2005).
67. Kim, S. *et al.* High-harmonic generation by resonant plasmon field enhancement. *Nature* **453,** 757–760 (2008).
68. Bouhelier, A., Beversluis, M. R. & Novotny, L. Characterization of nanoplasmonic structures by locally excited photoluminescence. *Appl. Phys. Lett.* **83,** 5041–5043 (2003).
69. Schuck, P., Fromm, D. P., Sundaramurthy, A., Kino, G. S. & Moerner, W. E. Improving the mismatch between light and nanoscale objects with gold bowtie nanoantennas. *Phys. Rev. Lett.* **94,** 017402 (2005).
70. Miller, D. A. B. Fundamental limit for optical components. *J. Opt. Soc. Am. B* **24**, A1–A18 (2007).
71. Alu, A. & Engheta, N. Input impedance, nanocircuit loading, and radiation tuning of optical nanoantennas. *Phys. Rev. Lett.* **101,** 043901 (2008).
72. Alu, A. & Engheta, N. Hertzian plasmonic nanodimer as an efficient optical nanoantenna. *Phys. Rev. B* **78,** 195111 (2008).
73. Olmon, R. L., Krenz, P. M., Jones, A. C., Boreman, G. D. & Raschke, M. B. Near-field imaging of optical antenna modes in the mid-infrared. *Opt. Express* **16,** 20295–20305 (2008).
74. Schnell, M. *et al.* Controlling the near-field oscillations of loaded plasmonic nanoantennas. *Nature Photon.* **3,** 287–291 (2009).
75. Taminiau, T. H., Stefani, F. D., Segerink, F. B. & van Hulst, N. F. Optical antennas direct single-molecule emission. *Nature Photon.* **2,** 234–237 (2008).
76. Hofmann, H. F., Kosako, T. & Kadoya, Y. Design parameters for a nano-optical Yagi–Uda antenna. *New J. Phys.* **9,** 217–217 (2007).
77. Li, J., Salandrino, A. & Engheta, N. Shaping light beams in the nanometer scale: A Yagi–Uda nanoantenna in the optical domain. *Phys. Rev. B* **76,** 245403 (2007).
78. Guo, H. *et al.* Optical resonances of bowtie slot antennas and their geometry and material dependence. *Opt. Express* **16,** 7756–7766 (2008).
79. Biagioni, P., Huang, J. S., Duò, L., Finazzi, M. & Hecht, B. Cross resonant optical antenna. *Phys. Rev. Lett.* **102,** 256801 (2009).
80. Esteban, R., Teperik, T. V. & Greffet, J.-J. Optical patch antennas for single photon emission using surface plasmon resonances. *Phys. Rev. Lett.* **104,** 026802 (2010).
81. Abdel-Rahman, M. R., Monacelli, B., Weeks, A. R., Zummo, G. & Boreman, G. D. Design, fabrication and characterization of antenna-coupled metal-oxide-metal diodes for dual-band detection. *Opt. Eng.* **44,** 066401 (2005).
82. Li, K., Stockman, M. I. & Bergman, D. J. Self-similar chain of metal nanospheres as an efficient nanolens. *Phys. Rev. Lett.* **91,** 227402 (2003).
83. Puente-Biliarda, C., Romeu, J., Pous, R. & Cardama, A. On the behavior of the sierpinski multiband fractal antenna. *IEEE T. Antenn. Propag.* **46,** 517–524 (1998).
84. Curto, A. G., Manjavacas, A. & de Abajo, F. J. G. Near-field focusing with optical phase antennas. *Opt. Express* **17,** 17801–17811 (2009).
85. Huang, C. *et al.* Gain, detuning, and radiation patterns of nanoparticles optical antennas. *Phys. Rev. B* **88,** 155407 (2008).
86. Huang, J.-S., Feichtner, T., Biagioni, P. & Hecht, B. Impedance matching and emission properties of nanoantennas in an optical nanocircuit. *Nano Lett.* **9,** 1897–1902 (2009).
87. Berthelot, J. *et al.* Tuning of an optical dimer nanoantenna by electrically controlling its load impedance. *Nano Lett.* **9,** 3914–3921 (2009).
88. Greffet, J.-J., Laroche, M. & Marquier, F. Impedance of a nanoantenna and a single quantum emitter. *Phys. Rev. Lett.* **105,** 117701 (2010).
89. Gimzewski, J. K., Reihl, B., Coombs, J. H. & Schlittler, R. R. Photon emission with the scanning tunneling microscope. *Z. Phys. B* **72,** 497–501 (1988).
90. Schull, G., Nel, N., Johanson, P. & Berndt, R. Electron–plasmon and electron–electron interactions at a single atom contact. *Phys. Rev. Lett.* **102,** 057401 (2009).
91. Johansson, P., Monreal, R. & Apell, P. Theory for light emission from a scanning tunneling microscope. *Phys. Rev. B* **42,** 9210–9213 (1990).
92. Persson, B. N. J. & Baratoff, A. Theory of photon emission in electron tunneling to metallic particles. *Phys. Rev. B* **68,** 3224–3227 (1992).
93. Zurita-Sanchez, J. R. & Novotny, L. Multipolar interband absorption in a semiconductor quantum dot. I. Electric quadrupole enhancement. *J. Opt. Soc. Am. B* **19,** 1355–1362 (2002).
94. Beversluis, M. R., Bouhelier, A. & Novotny, L. Continuum generation from single gold nanostructures through near-field mediated intraband transitions. *Phys. Rev. B* **68,** 115433 (2003).
95. Shalaev, V. M., Douketis, C., Haslett, T., Stuckless, T. & Moskovits, M. Two-photon electron emission from smooth and rough metal films in the threshold region. *Phys. Rev. B* **53,** 11193–11206 (1996).
96. Ditlbacher, H. *et al.* Silver nanowires as surface plasmon resonators. *Phys. Rev. Lett.* **95,** 257403 (2005).
97. Averitt, R. D., Sarkar, D. & Halas, N. J. Plasmon resonance shifts of Au-coated Au_2S nanoshells: Insight into multicomponent nanoparticle growth. *Phys. Rev. Lett.* **78,** 4217–4220 (1997).
98. Bharadwaj, P. & Novotny, L. Plasmon-enhanced photoemission from a single $Y_3N@C_{80}$ fullerene. *J. Phys. Chem. C* **114,** 7444–7447 (2010).
99. Huang, J.-S. *et al.* Atomically flat single-crystalline gold nanostructures for plasmonic nanocircuitry. *Nature Comm.* **1,** 150 (2010).
100. Challener, W. A. *et al.* Heat-assisted magnetic recording by a near-field transducer with efficient optical energy transfer. *Nature Photon.* **3,** 220–224 (2009).
101. Stipe, B. C. *et al.* Magnetic recording at 1.5 Pb m^{-2} using an integrated plasmonic antenna. *Nature Photon.* **4,** 484–488 (2010).

Acknowledgements

N.L. and N.v.H. thank C. Hoeppener and P. Bharadwaj for providing the particle trimer probe shown in Fig. 5a. They also thank T. Taminiau for valuable discussions. N.L. and N.v.H. thank M. Castro-Lopez, G. Volpe, L. Neumann, A. Curto, M. Kuttge and R. Quidant for providing several top-down fabricated antennas. L.N. acknowledges financial support from the US Department of Energy (DE-FG02-01ER15204) and the National Science Foundation (ECCS- 0918416 and ECCS-0651079). N.v.H. thanks the Spanish Ministry of Science and Innovation (CSD2007-046-NanoLight.es and FIS2009-08203), the Fundacio Cellex Barcelona and the European Research Council (AdvGrant ERC247330) for financial support.

Additional information

The authors declare no competing financial interests.